Chemistry–A European Journal
Research Article
doi.org/10.1002/chem.202301767
Chemistry Europe
European Chemical Societies Publishing
www.chemeurj.org

The Power of Automation in Polymer Chemistry: Precision Synthesis of Multiblock Copolymers with Block Sequence Control

Vianna F. Jafari,[a] Zahra Mossayebi,[a] Stephanie Allison-Logan,[a] Sadegh Shabani,[a] and Greg G. Qiao*[a]

Machines can revolutionize the field of chemistry and material science, driving the development of new chemistries, increasing productivity, and facilitating reaction scale up. The incorporation of automated systems in the field of polymer chemistry has however proven challenging owing to the demanding reaction conditions, rendering the automation setup complex and costly. There is an imminent need for an automation platform which uses fast and simple polymerization protocols, while providing a high level of control on the structure of macromolecules via precision synthesis. This work combines an oxygen tolerant, room temperature polymerization method with a simple liquid handling robot to automatically prepare precise and high order multiblock copolymers with unprecedented livingness even after many chain extensions. The highest number of blocks synthesized in such a system is reported, demonstrating the capabilities of this automated platform for the rapid synthesis and complex polymer structure formation.

Introduction

The implementation of automation and machine-learning (ML) for scientific discoveries has opened a new era of technological advancement. The record-breaking development and production of COVID-19 vaccines with the help of automation and ML algorithms signifies the importance of this paradigm shift in scientific discoveries.[1] In the field of material science, ML algorithms require access to reliable and high-quality training data to learn the underlying patterns and successfully predict the desired structures and/or properties. Relying only on academic literature for this purpose poses the algorithms to a bias towards successful experiments, while ML algorithms require a wide range of successful and unsuccessful data to build a more powerful problem-solving model.[2] In this context, automation and high throughput (HTP) experimentation can provide a comprehensive set of data by rapidly evaluating many possible chemistries.[3] Accordingly, the field of polymer chemistry has attracted the use of machines to automate polymerization processes in recent years.[4,5] The vast chemical space of possible polymer structures and compositions can benefit from the efficiency and accuracy of automation technologies, while producing high quality experimental data for ML algorithms.[6] The automated, self-optimizing flow system employed by Junker's group[7] to prepare polymers with targeted molecular weights and monomer conversions demonstrates the direction towards which the future of smart polymer synthesis platforms is headed. A more comprehensive review of these recent trends of automation and ML in polymer science has been published by Martin et. al[8]

Among various polymerization techniques, reversible-deactivation radical polymerizations (RDRP) including atom transfer radical polymerization (ATRP) and reversible addition-fragmentation chain-transfer (RAFT) have attracted attention for automation purposes as they provide exquisite control on the MW and structure of polymers, while offering systems compatible with an unparalleled range of monomers and architectures with applications in drug delivery systems, surfactants, gas separation mechanisms, data storage and DNA replication.[9] These advantages make RDRP systems promising candidates for HTP experimentations to study structure-property relationships in polymers and to produce large datasets. However, many of these polymerization techniques still suffer from oxygen sensitivity, long reaction times, high cost of specialized reagents, and the requirement for external stimuli to activate the polymerization reaction. These factors limit the accessibility of automation tools for these systems.[10,11]

To facilitate access to automated platforms for the creation of complex polymer structures, an ideal polymerization technique would have to meet the following criteria: 1) oxygen tolerance, 2) fast reactions reaching high monomer conversion within a reasonable amount of time, 3) control of molecular weight (MW) and polymer chain structure, and 4) high livingness of chains.

[a] V. F. Jafari, Z. Mossayebi, Dr. S. Allison-Logan, Dr. S. Shabani, Prof. G. G. Qiao
Department of Chemical Engineering
The University of Melbourne
Parkville, VIC 3010 (Australia)
E-mail: gregghq@unimelb.edu.au

Supporting information for this article is available on the WWW under https://doi.org/10.1002/chem.202301767

Liquid handling robots have recently been used to automate polymer synthesis that meet the above-mentioned criteria. Gormley et. al[5] have utilized oxygen tolerant photo-induced electron/energy transfer RAFT (PET-RAFT) and thermally initiated Enzyme-RAFT to automatically synthesize acrylamide class homopolymers and pseudo-triblock copolymers with excellent control on MW and livingness. In a more recent work by the same group,[12] automated oxygen-tolerant PET-RAFT was conducted using a custom-designed lightbox to control individual reactions in a well-plate. Series of homopolymers and random copolymers with different compositions were synthesized and characterized online using fluorescence reading. PET-RAFT has also been used in another recent work by Foster et. al[13] to automatically prepare multiblock star copolymers, studying the effect of block composition on the star properties. However, these platforms require an external stimulus in the form of light or heat to initiate polymerization, while not all cases produce complex polymeric structures. A system that does not require an external stimulus for the activation of the polymerization reaction is preferred since it simplifies the reaction setup for automation and expands the scale at which the reaction can be performed. To date, no automated system has been reported that incorporates all the criteria mentioned above, including no need for external stimuli, while producing complex polymeric structures that bear significance for further studies.

To address the complexities and requirements of a reliable RDRP technique for automation, we focused on the synthesis of high order multiblock copolymers[14,15] – macromolecular chains into which different monomers are imbedded as homopolymeric segments.[16] This class of polymers provides a versatility of blocks with different chemistries, which enables the polymer chains to exhibit new properties not observed in conventional homopolymers or random copolymers. As alluded to by Bates et al., block copolymers, their synthesis and applications have evolved over more than 60 years since their inception.[17] Sequence-controlled multiblock copolymers can self-fold and mimic naturally folding biomaterials,[18] with potential to act as high-capacity data storage platforms or exhibit biological benefits in biomedical applications.[19] However, the many possible structures with different monomers, block numbers and block lengths cannot be thoroughly investigated manually. Therefore, automation and high-throughput (HTP) experimentation can play crucial roles in streamlining the discovery of structure-property relationships of multiblock copolymers to provide output at a higher capacity.[11,20] While a plethora of complex block copolymers have been synthesized and evaluated using different chemistries usually sensitive and labor-intensive,[21] we were interested in devising an RDRP system that facilitates their preparation in a one-pot setup which offers fast reaction speeds, oxygen tolerance, and high livingness at room temperature, enabling the automation of such a system to achieve block numbers beyond the current limitation.[22]

In this work we present an automated, oxygen tolerant RDRP at room temperature, employing our previously reported semi bio-Fenton RAFT polymerization[23] to prepare high order multiblock copolymers, exhibiting unprecedented livingness in an open-to-air system without the need for external stimuli for activation. The choice of the automation system in this work reflects the importance of the availability of these platforms, as well as the need for simplicity and less customized robotic systems. The batch operation mode of the automation system chosen here is also preferred to flow systems, since flow reactors require customization to suit most chemical reactions performed conventionally in batch systems.[24] A small polymer library is also synthesized using the automation platform to systematically vary block numbers, lengths and sequences to elucidate the effect of these factors on the properties of polymers evaluated using Dynamic Light Scattering (DLS). To show the robustness of this automated system, we also report for the first time the synthesis of a polymer chain with 39 blocks in a room-temperature, open-to-air setup, while providing excellent livingness.[22]

Results and Discussion

Optimization of semi bio-Fenton RAFT polymerization for high block numbers

Our team has previously pioneered the development of semi bio-Fenton RAFT polymerization, which employs mild reaction conditions and offers oxygen tolerance to prepare polymers with very high livingness and control of molecular weight (MW).[23] In this technique, the use of glucose oxidase (GOx) enzyme coupled with ferrous ions (Fe^{2+}) can provide a dual-role initiating mechanism *(*Figure 1*)*. GOx utilizes O_2 present in the solution, effectively degassing the system, to produce hydrogen peroxide, which in turn is transformed into hydroxyl radicals through a thermodynamically favored Fenton redox reaction employing Fe^{2+}. The mild condition of this reaction offers simplicity in terms of setup – no need for oil baths, light sources, or thermocyclers – which essentially provides a green bench-top setup that can be used in any laboratory with minimum requirements. The reaction is performed at room temperature, which minimizes unfavored side reactions. In

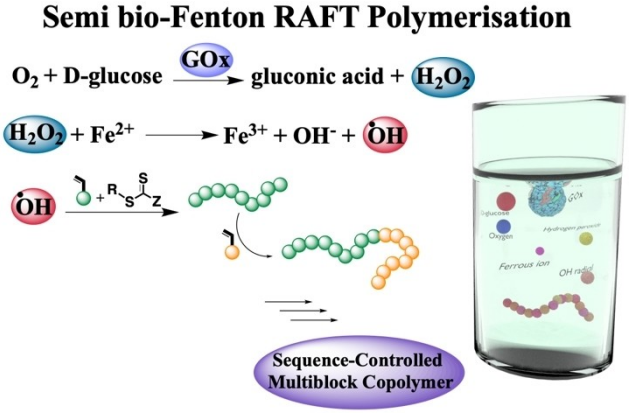

Figure 1. Depiction of the semi bio-Fenton RAFT reaction performed in the presence of air at room temperature, to produce high order, sequence-controlled multiblock copolymers.

addition, the mild conditions of this polymerization system can provide a suitable means to investigate polymeric structures in biological environments where the use of a light or heat source is challenging.[25] Achieving ultra-high molecular weight polymers using the semi bio-Fenton RAFT chemistry in a previous work by our group was indicative of the high livingness of chains,[26] which led us to investigate the capability of this method for the automated synthesis of high-order multi-block copolymers, where chain-end fidelity plays an essential role in achieving such complex structures. To this end, a series of optimization experiments were performed initially to ensure high livingness, fast reaction, and versatility is achieved with this polymerization technique.

In a typical semi bio-Fenton RAFT polymerization setup, *N,N*-Dimethylacrylamide (DMA) was polymerized in a RAFT system using *S,S′*-Bis(α,α′-dimethyl-α″-acetic acid)-trithiocarbonate (TTC) as the RAFT agent in deionized water as solvent. Different concentrations of semi bio-Fenton RAFT reagents were investigated for the best kinetic results using DMA, while using minimal amounts of reagents, affording a green chemistry which will also justify commercial scale synthesis *(*Figure 2 *and Table S1)*. Ultimately, semi bio-Fenton RAFT reagents were used at the following concentrations: ammonium ferrous sulfate hexahydrate (iron source, 1 mM), glucose oxidase (2 μM), D-glucose (excess). This system yielded a highly controlled polymer with narrow molecular weight distribution and excellent control on the targeted MW ($M_{n,theo}$ = 10.2 kg mol^{-1}, $M_{n,SEC}$ = 11.8 kg mol^{-1}, Đ = 1.1). Interestingly, adding higher amounts of ferrous ion had an adverse effect, terminating the chains pre-maturely and resulting in a non-symmetrical distribution in GPC *(*Figure 2b*)*. This can be attributed to a higher radical flux when more ferrous ions are available to convert available H_2O_2 to hydroxyl radicals.

To show the versatility of this method for different automation options, various common labware were used to prepare pDMA linear polymers ($M_{n,theo}$ = 10.2 kg.mol^{-1}) at room temperature with no degassing and no stirring in different reaction sizes ranging from 500 mL to 3 mL using the optimized reagents concentrations. These included multi-well plates, PCR tubes, and glassware with various sizes and geometries. Semi bio-Fenton RAFT polymerization provided controlled and rapid reaction (1 h) at room temperature for all these different labware, resulting in narrow polydispersity (Đ < 1.2). *(Figure S1 and Table S2)*

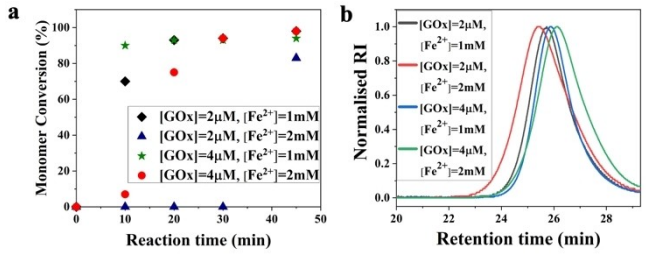

Figure 2. Optimization of reagents concentrations in the semi bio-Fenton RAFT polymerization of $pDMA_{100}$. (a) Kinetic study of four different reaction conditions showing monomer conversion with time, reactions stopped at 45 min. (b) Molecular weight distribution (GPC) of all four variants.

Having established the optimum reagents concentrations for the semi bio-Fenton RAFT technique in water, we investigated the manual one-pot synthesis of multi-block copolymers in preparation for the automation protocol. With longer reaction times in a one-pot multiblock synthesis procedure, the production of gluconic acid *(Figure S2)* must be taken into account. The accumulation of gluconic acid over time decreases the pH of the solution, while pH is known to affect both Fenton reactions and the activity of GOx enzyme.[27] To ensure optimum conditions for these two factors, pH 5.5 was maintained for this system using 0.1 M acetate buffer as the reaction medium (prepared by mixing adequate amounts of sodium acetate and acetic acid) which shows acceptable tolerance towards the production of gluconic acid at pH 5.5 when used as solvent instead of H_2O.

Manual preparation of multi-block copolymers using semi bio-Fenton RAFT

Before we investigate if an automation platform can facilitate the synthesis of complex polymeric structures, we first investigated the manual preparation of multiblock copolymers to show the versatility of semi bio-Fenton RAFT polymerization for both automated and manual synthesis protocols. To this end, we first worked on the one-pot sequential synthesis of pDMA pseudo-block copolymers (DP_{blocks} = 25) without degassing at room temperature using a stirrer plate. Sequential monomer addition was performed without any intermediate purification. The starting reaction volume was 2 mL. 11 chain extensions (23 blocks) were achieved in only 8 h with each chain extension taking 40 min to reach near quantitative monomer conversion. The high level of chain end fidelity was evident from the narrow polydispersity of polymer samples throughout the reaction (starting from 1.02 and ending with 1.04 for the final sample containing 23 pseudo-blocks) (Table S3), as well as no visible tailing or non-symmetrical distributions in the GPC peaks (Figure S3b). The slight difference between theoretical and measured MW can be attributed to unavoidable errors in measurement – instrument error while adding reagents (balances and pipettes), as well as the volume change of the reaction solution that occurs when samples are taken for GPC and NMR analysis throughout the reaction. An overlay of GPC peaks for all chain extensions showed a clear shift to the higher MW range (lower retention time in SEC columns) that was proof of the livingness of chains and the MW growth after each chain extension. (Figure S3)

After the successful synthesis of pDMA pseudo-block copolymers, we moved on to prepare complex multiblock copolymers using two different monomers – DMA and 4-Acryloylmorpholine (NAM) – in a one-pot sequential system. No intermediate purification was performed, and the reaction was carried out at room temperature without degassing. Analyzed data showed a high level of control provided by semi bio-Fenton RAFT polymerization to make polymers with 23 blocks

($DP_{block} = 25$) while still preserving chain-end fidelity and low dispersity ($Đ_{23\ blocks} = 1.08$) (Table S4). The measured MW was in agreement with the theoretical value for all chain extensions which showed the capability of this technique to accurately design and prepare polymers with a high number of blocks (Figure 3b). An overlay of GPC peaks for all chain extensions showed a clear shift to the higher MW range, proving that chains preserved their livingness throughout the chain extension steps in the reaction, while maintaining a fast polymerization rate at room temperature (Figure 3a), reaching quantitative monomer conversion for all chain extension steps (Figure S4). The reaction scheme for the preparation of multiblock copolymers and the structure of the final 23-block copolymer can be seen in Scheme 1.

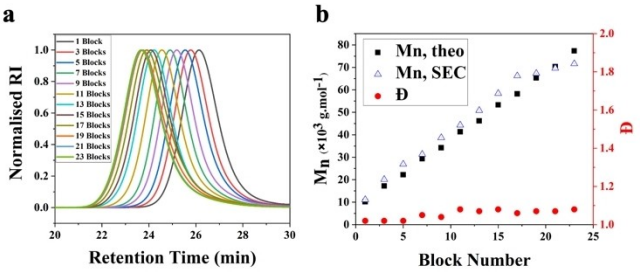

Figure 3. Multiblock copolymers prepared manually using semi bio-Fenton RAFT, with the 23-block copolymer structure shown in scheme 1. (a) Overlay of molecular weight distributions (GPC) of one-pot sequential chain extension reactions. (b) Comparison of theoretical and measured number average molecular weight, and the evolution of polydispersity (Đ) with block number.

After successfully achieving highly living multiblock copolymers in an open to air, room temperature system, we moved on to the automation phase. The automation setup selected for this work is a commercially available liquid handling robot (OT-2 robot), primarily designed for biological applications. The first stage of the work involved developing a method for the use of this robot for polymerization reactions.

Method development for the use of the robot for polymerization reactions

Four steps are required to employ the liquid handling robot for the execution of polymerization reactions: protocol design, labware definition, programming the computer interface, and automated synthesis, as shown in Figure 4.

1) **Protocol Design**: In this step, the Protocol Designer tool is used to add a step-by-step protocol, detailing the actions of the pipettes, including the amount and type of liquid to be transferred, the speed of withdrawal and dispensing of liquids, as well as any pause durations required throughout the experiment. Using the Protocol Designer tool, the deck state at each reaction step can be viewed and controlled, and information including the volume and contents of each container are also available.
2) **Labware Definition**: In this step, all the labware intended to be used on the deck of the robot will be introduced to it through specifying the dimensions and types of labware. To overcome the shortfall of this robot's "less customizable"

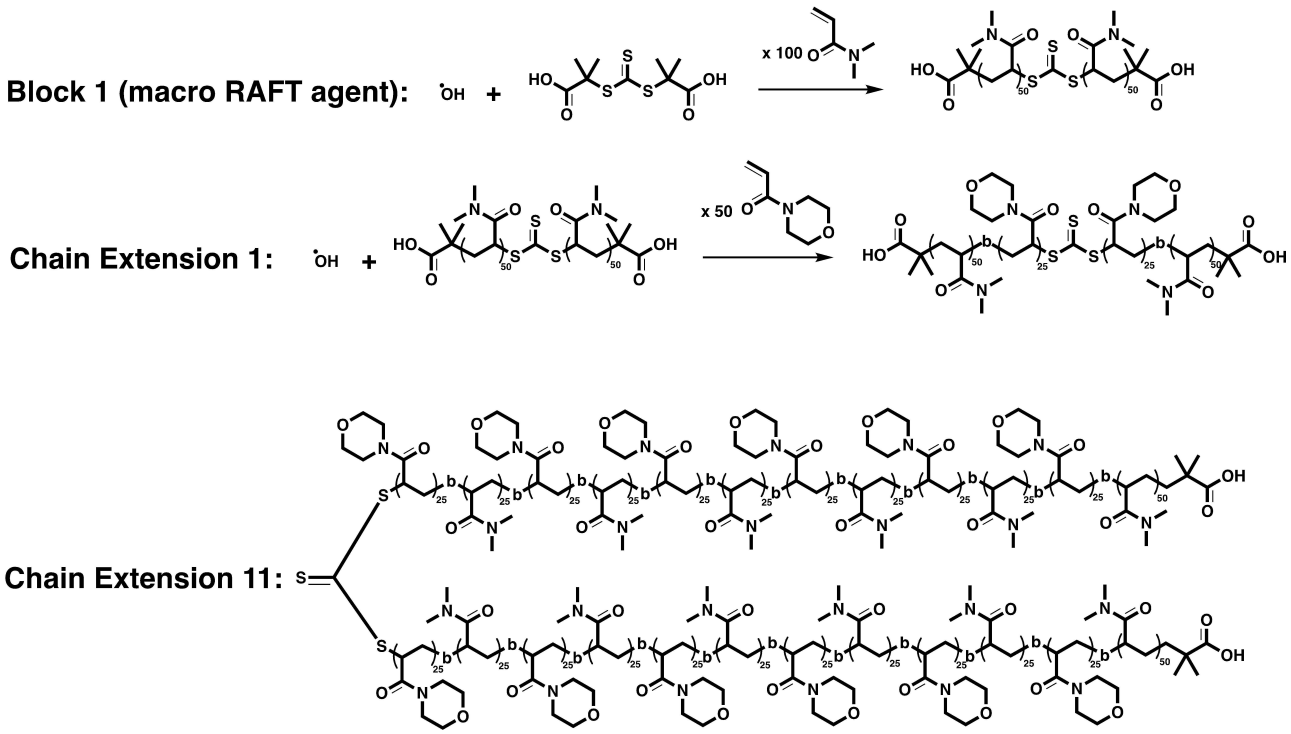

Scheme 1. Reaction scheme for the manual one-pot preparation of multiblock copolymers via the semi bio-Fenton RAFT technique, resulting in a 23-block copolymer: $pDMA_{50}$-*b*-$pNAM_{25}$-*b*-$pDMA_{25}$-*b*-$pNAM_{25}$-*b*-$pDMA_{25}$-*b*-$pNAM_{25}$-*b*-$pDMA_{25}$-*b*-$pNAM_{25}$-*b*-$pDMA_{25}$-*b*-$pNAM_{25}$-*b*-$pDMA_{25}$-*b*-$pNAM_{50}$-*b*-$pDMA_{25}$-*b*-$pNAM_{25}$-*b*-$pDMA_{25}$-*b*-$pNAM_{25}$-*b*- $pDMA_{25}$-*b*-$pNAM_{25}$-*b*- $pDMA_{25}$-*b*-$pNAM_{25}$-*b*- $pDMA_{25}$.

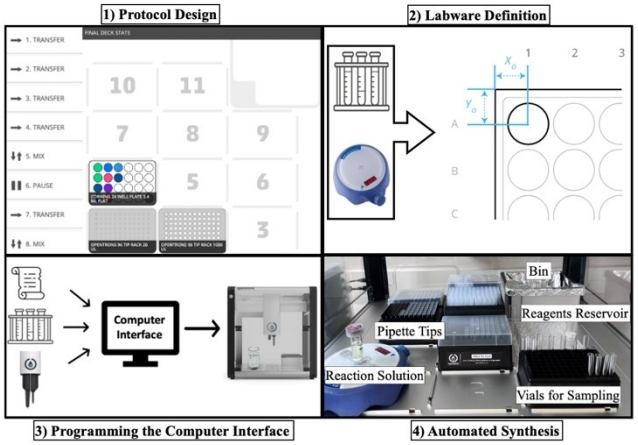

Figure 4. Main four steps employed to conduct semi bio-Fenton RAFT polymerization reactions in the automated platform.

character,[28] we manipulated the calibration process and labware definition steps to implement a magnetic stirrer plate into the robot, as well as fashioning common labware to be used as vial holders of different sizes. This eliminated the need for additional modules and machine-specific labware. The ability to customize the deck of the robot can also help with the incorporation of chemistries requiring external stimuli, where it would otherwise be necessary to have access to modules including the Thermocycler and Temperature modules.

3) **Programming the Computer Interface**: The reaction protocol and labware definition files are then uploaded into the Opentrons application, which is run on a computer connected to the robot. The app runs the protocol and performs calibration processes on the deck and connected pipettes, ensuring that all parts of the machine are suitably positioned to successfully conduct the experiment.
4) **Automated Synthesis**: In this step, the robot runs the intended protocol in a fully autonomous mode. Similar to most automated systems, an operator will still need to fill reagent reservoirs and remove finished reaction solutions and analysis samples from the deck.

Automated synthesis of multi-block copolymers using semi bio-Fenton RAFT

To prepare high order multiblock copolymers using the automation platform, a glass vial with a magnetic stirrer bar was placed on the stirrer plate occupying two slots on the robot deck. Monomers and D-glucose stock solution in glass vials were placed on a 24-well plate acting as a vial rack. Small glass vials were also placed on an empty pipette-tip holder for NMR and GPC sample retrieval, with acetone in GPC sample vials for polymer precipitation, and a solution of hydroquinone in deuterated water (200 mM) for NMR samples, both to stop further reaction of the polymer chains in the sample. In addition, a vial lid with rubber membranes was designed for use in the experiment. While semi bio-Fenton RAFT polymerization offers an oxygen-tolerant system, it is preferred to put a lid on the reactor when no liquid transfer is being conducted to offer a relative seal. This is done to prevent excess oxygen from entering the headspace of the reactor, causing unwanted reactions or induction periods, as well as reducing the evaporation since the reaction goes for many hours. The lid bears crosshairs on the membrane, allowing an acceptable seal for the reaction occurring in the glass vial, while providing an opening for the pipette tips to be inserted for monomer additions, dilutions, and sample retrievals. (Figure S5)

Using the Protocol Designer tool (Figure S6), all the steps of chain extension and sample retrieval were designed. The initial reaction solution (block 1) was prepared manually and placed on the stirrer plate. The starting reaction volume was 2 mL, with a large headspace above the reaction (Figure S3d). This large headspace did not adversely affect the livingness of polymer chains which indicates the high effectiveness of semi bio-Fenton RAFT polymerization in retaining chain end functionality. Using the OT-2 robot desktop application on a computer, the desired protocol was run and chain extensions up to 19 (39 blocks, considering the symmetrical nature of the RAFT agent, allowing blocks to form on both sides of the macro-RAFT agent) were performed. Considering the high number of chain extensions performed in each reaction, analysis samples were taken at longer chain extension intervals to avoid a significant change in the concentration of semi bio-Fenton reagents, as well as polymer chains bearing the RAFT agent. Table 1 summarizes the analysis data of these samples. Analysis of samples taken automatically by the robot shows a clear shift to the higher MW values in GPC analysis with no tailing (Figure 5a), while maintaining narrow polydispersity (Figure 5b) indicating the excellent capability of this system to retain livingness of polymer chains even after such high chain extension numbers. Due to the increase in viscosity, further chain extensions were not performed. However, the high livingness observed in the 39-block sample shows that with optimized reaction conditions or dilution of the sample, achieving higher numbers of blocks are still possible.

To show the repeatability of this automated multiblock synthesis setup, three sets of multiblock copolymers with the backbone structure p(DMA_{50}-b-NAM_{12}-b-DMA_{12}-b-NAM_{12}-b-DMA_{25}-b-NAM_{12}-b-DMA_{12}-b-NAM_{12}-b-DMA_{50}) were prepared within a timespan of several weeks. Results obtained from the GPC analysis of these multiblock copolymers successfully demonstrates the capability of the machine to produce repeatable and reliable data when experiments are conducted at different times. (Figure S7 and table S5)

The 39-block copolymer prepared in less than 24 h using the automated setup, as well as the 23-block copolymer prepared manually, show an excellent retention of chain-end fidelity in the semi bio-Fenton RAFT system evident from the narrow polydispersity even at a high block number. This polymerization technique yields high-conversion polymers at each chain extension iteration, while providing control on the MW and chain-end fidelity. This is done at room temperature in an open-to air system, making the synthesis of complex

Table 1. Summary of block copolymers synthesized and sampled automatically by the automation platform. Reaction time: 60 min per chain extension, (pDMA)-co-(pNAM) multi-blocks with DP for each block = 12 (×2 for each chain extension cycle), [GOx] = 2 mM, [Fe^{2+}] = 1 mM, [Glucose] = excess.

Chain Extension Cycle (DP_{block})	$M_{n,theo}$ (10^3 g.mol^{-1})[a]	$M_{n,SEC}$ (10^3 g.mol^{-1})[b]	Đ[c]	Conversion (%)[d]	Block number	Polymer Chain Structure[e]
0 (100)	10.2	11.5	1.06	> 99	1	
2 (12)	16.2	19.5	1.03	> 99	5	
7 (12)	31.7	25.2	1.07	> 99	15	
10 (12)	40.2	33.7	1.05	> 99	21	
13 (12)	49.8	39.3	1.05	> 99	27	
16 (12)	58.2	46.5	1.08	> 99	33	
19 (12)	64.3	54.1	1.06	> 99	39	

[a] Calculated using the following formula: $M_{n,theo} = DP \times Conversion \times MW_{Monomer} + MW_{RAFT\ agent}$. [b,c] Calculated from Aqueous GPC/SEC. [d] Determined via ^{1}H NMR analysis. [e] Each red circle represents 12 repeating units of DMA, and each blue circle 12 repeating units of NAM.

multiblock copolymers available to most research laboratories where these materials can be investigated for beneficial properties.

Assembly behavior of sequence-controlled multiblock copolymers:

It is well established that block copolymers with limited number of blocks (generally 5 or less) form assemblies with different morphologies in selective solvents (i.e, solvents dissolving one block and not the other) which bring advantages for a wide range of applications in biomaterials, electronics, catalysts, etc. and this has been studied extensively over the past few decades.[29] The selection of solvent plays an important role in the solution behavior of block copolymers. Non-soluble segments of the block copolymer collapse, resulting in different assembly sizes.[30] Having demonstrated the capability to synthesize sequence-controlled multiblock copolymers with high livingness, we set out to investigate the effect of higher block numbers on the self-assembly and solution behavior of copolymers by designing and preparing a library of polymers (Table 2, Figure S8) using the automation platform. To this end, a library of 9 different polymers with similar MW[31] were prepared using two different monomers, DMA and NAM, that can be categorized into three groups. Group 1 (polymers A and B) consisted of homopolymers of DMA and NAM respectively. Group 2 (polymers C–H) included multiblock copolymers of DMA and NAM, bearing 3 blocks (C and D), 7 blocks (E and F), and 17 blocks (G and H), with varying block lengths and block sequences while keeping the overall MW and monomer composition constant. Lastly, group 3 consisted of a random copolymer (I) with a similar monomer composition and MW to polymers of group 2, without any block sequence control. A kinetic study of the random copolymer synthesis showed that both monomers were consumed at a relatively similar rate (Figure S9), indicating a true random distribution of both monomers for polymer I chain structure. The random copolymer synthesis was performed three times to ensure repeatability (Table S6). All polymers in the library exhibited a narrow polydispersity (< 1.2) and near quantitative monomer conversion (Table S6). These polymers were then dissolved in water, methanol, and ethanol respectively and were tested via Dynamic Light Scattering (DLS) to study their assembly behavior. To rule out the effect of concentration on the morphology of aggregates,[32] all DLS experiments were initially performed at a concentration of 10 mg/mL.

As water is a nonselective solvent for both pDMA and pNAM, all polymers regardless of their block sequences were readily dissolved in water and yielded clear solutions with a particle size (PS) ranging from 7.72 to 9.86 nm (Table 2). It is hypothesized that the block copolymer chains are unimolecularly present in water with slightly bigger PS due to the stretching of the chains in a good solvation state.[31,33] However, random copolymer showed a slightly smaller PS, possibly due to tight unimolecular packing.

Methanol and ethanol are both selective solvents for pDMA.[34] This was confirmed by the visual inspection of the samples prepared from pDMA and pNAM homopolymer (polymers A and B respectively) with the former readily dissolving and the latter not dissolving in either solvent.

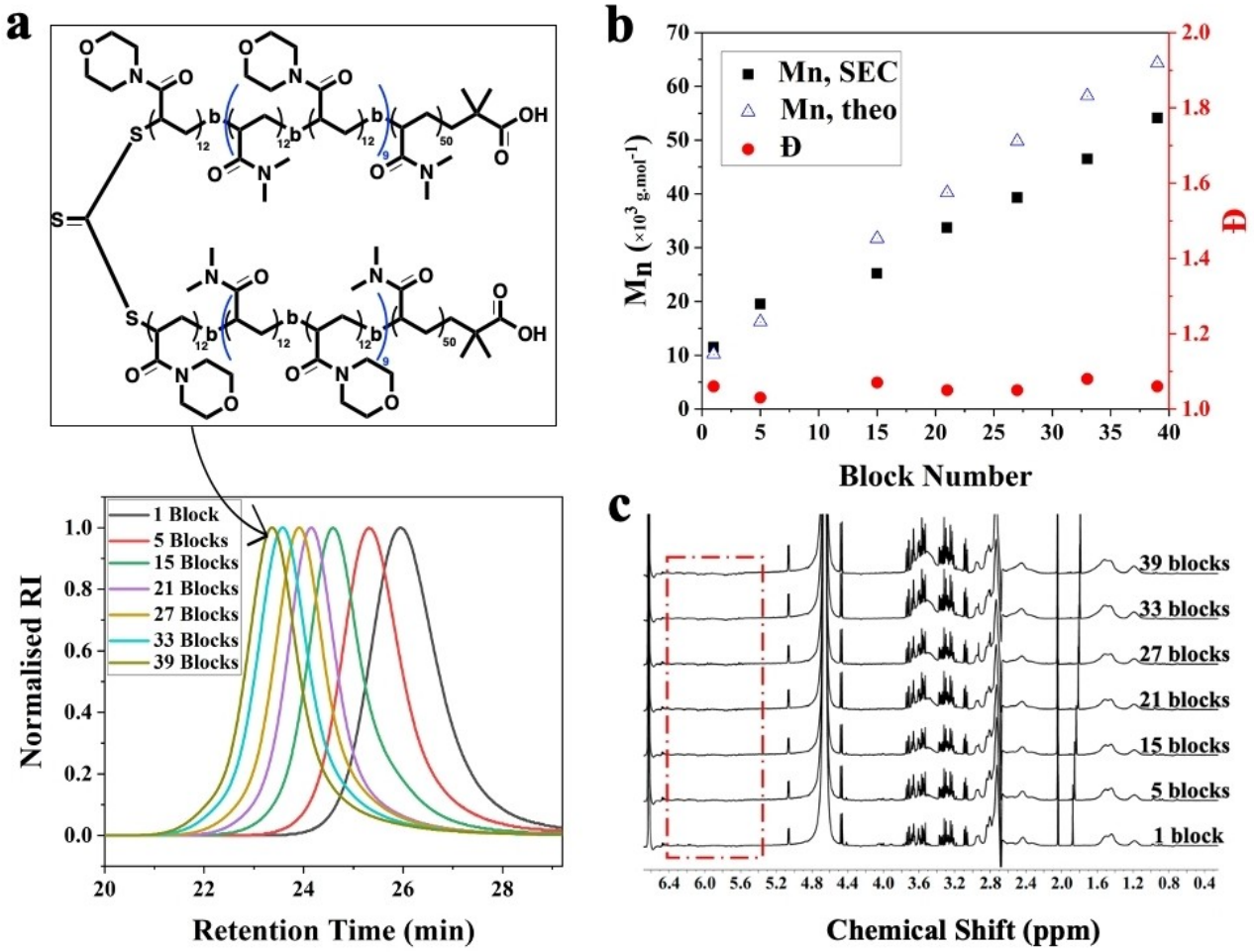

Figure 5. Highest number of blocks prepared in a one-pot, automated, open-to-air system. (a) Overlay of MW distributions of block copolymers sampled throughout the reaction along with the structure of the final 39-block copolymer. (b) Comparison of theoretical and measured number average molecular weight, and the evolution of Đ with block number. (c) ^{1}H NMR spectra retrieved from different block copolymers sampled automatically throughout the reaction

With MeOH as the solvent, polymer A showed a PS of 10.60 nm, hinting to an expanded unimolecular chain in solution. Polymer B was insoluble in MeOH, but when a long pDMA block was inserted in the middle of the chain (polymer C, 3 blocks), the chains were dissolved and showed a PS of 33.34 nm. Polymer D which has the same monomer composition and block number as C, only with the block sequence reversed, also showed a PS of 30.41 nm, showing that both C and D have formed multi-chain assemblies in MeOH. Cutting the block lengths in half and creating 7-block copolymers (E and F) resulted in a drop in PS, which stayed relatively constant after further cutting of the inner blocks in half for polymers G and H (17-block copolymers), showing that an increase in block number and decrease in block length have resulted in the disruption of assemblies, where it is hypothesized that 1–2 chains are assembled into particles. Radom polymer I also showed similar PS to copolymers with high block numbers.

Changing the selective solvent to EtOH however showed more interesting structure-property differences. Firstly, triblock copolymer C bearing two insoluble pNAM blocks on both ends of the chain did not dissolve in EtOH at 10 mg/ml, as EtOH is a poorer solvent for pNAM. Secondly, all the copolymers showed a larger PS in EtOH, hinting to the fact that there are more assemblies forming in EtOH compared to MeOH. Polymers E and F, both having 7 blocks with similar monomer composition, showed different PS solely because of their block sequence difference. Polymer E has a soluble pDMA block in the middle of the chain which has increased PS because of expansion in a good solvent. 17-block copolymers G and H showed self-assembly behavior, while their equivalent random copolymer I showed a significantly small PS of 6 nm, indicating the presence of single chains in solution with no aggregate-forming behavior.[33]

Polymers in this library were then dissolved at higher concentrations to further evaluate solubility and assembly behavior in EtOH (Table S7). An increase in PS for all variants except polymer A was observed. It is hypothesized that polymer A stayed in a molecular form due to the solubility of pDMA chains in EtOH. The increase in PS for multiblock copolymers (D to H) by changing the concentration further confirms the presence of assemblies interacting with the selective solvent EtOH. An increase in the PS of the random copolymer I was also

Table 2. Summary of polymer library prepared via the automated semi bio-Fenton platform for assembly behavior study.

Group	Variant	Chain structure[a]	Block number	$M_{n,SEC}$ (10^3 g.mol^{-1})	Đ	End block (DP)[b]	Middle block (DP)	Particle size in water (nm)[c]	Particle size in methanol (nm)	Particle size in ethanol (nm)
1 Homo-polymers	A		1	43.2	1.15	–	–	9.06	10.60	10.02
	B		1	46.0	1.09	–	–	8.60	Insoluble	Insoluble
2 Block Copolymers	C		3	49.2	1.11	pNAM (100)	pDMA (200)	9.37	33.34	Insoluble
	D		3	52.0	1.11	pDMA (100)	pNAM (200)	9.25	30.41	37.29
	E		7	46.0	1.06	pNAM (50)	pDMA (100)	9.86	10.66	23.45
	F		7	45.8	1.05	pDMA (50)	pNAM (100)	9.32	10.26	15.75
	G		17	43.5	1.11	pNAM (50)	pNAM (25)	8.36	10.58	15.08
	H		17	47.8	1.12	pDMA (50)	pDMA (25)	8.94	9.81	16.75
3 Random Copolymer	I	*Random*	–	43.5	1.16	–	–	7.72	8.78	6.06

[a] In the polymer chain structure, black circles represent the symmetrical RAFT agent (not including the R end groups), red circles represent 12–13 units of NAM and blue circles represent 12–13 DMA units respectively. No chain structure is depicted for the random copolymer I as this variant was not sequence controlled. [b] End blocks reside on both ends of the symmetrical polymer chain, outside the green dashed box. [c] Particle size measurements via DLS are performed at a solution concentration of 10 mg/mL with each PS number representing an average of three measurement.

observed. However, the size obtained from these samples (9.93 nm) still suggests that random copolymers are present in a unimolecular form, incapable of forming assemblies in EtOH in comparison to their equivalent 17-block copolymers. One may expect that using complex solvent systems and additives will further affect the assembly behavior of these block copolymers.[35]

It is evident from these experiments that a random copolymer exhibits a different behavior compared to its equivalent 17-block copolymers in a selective solvent. With the sequence which can be swiftly altered by design using the automated synthesis platform presented in this work, there still remains the possibility that even at very small block lengths, a wide range of high-order multiblock copolymers resembling that of complex natural polymers can be made.[15,36] These structures are different from a random copolymer structure and thus can provide a new tool for designing polymers with versatile monomer/block sequences.

Conclusions

In this work, we have established a fast and accurate automated synthesis platform for the preparation of sequence-controlled multiblock copolymers, offering a room-temperature and oxygen-tolerant reaction condition. The high livingness offered by the semi bio-Fenton RAFT technique in conjunction with the automated synthesis platform enabled us to make high order multiblock copolymers difficult to prepare manually. We were also able to show that by changing the block sequence, copolymers exhibited different physical properties. The future perspective for this work is to harness the precision offered by this automation platform to prepare more diverse and complex polymeric architectures, as well as integrating online characterization tools to create comprehensive structure-property datasets that can be later used for the training of machine learning algorithms to predict polymer properties and structures. A paradigm shift in the field of material science is eminent and automation platforms such as the one presented in this work can be considered as foundational work to build the capabilities to accommodate this shift towards more efficient and smart material design.

Experimental Section

Materials: GOx from Aspergillus niger was purchased from Sigma-Aldrich and used as received. Monomers N,N-dimethylacrylamide (DMA, 99%) and 4-acryloylmorpholine (NAM) were purchased from Sigma-Aldrich and de-inhibited by passing through inhibitor removers and/or basic alumina prior to use. D-glucose (99.5%, BDH), ammonium ferrous sulfate hexahydrate ($(NH4)_2Fe(SO4)_2 \cdot 6H2O$, Uni Lab Co.), RAFT agent TTC (S,S0-Bis(α,α′-dimethyl-α″-acetic acid)-trithiocarbonate, Boron Molecular), sodium acetate (Thermo Fisher Scientific) and acetic acid (ChemSupply Australia) were all used as received.

Manual preparation of multiblock copolymers using semi bio-Fenton RAFT Polymerization: In a typical semi bio-Fenton RAFT

polymerization, 2 mmol DMA (0.198 g) and 0.02 mmol TTC (0.0056 g) were mixed in a 7 mL glass vial, then stock solutions containing 0.4 mmol D-glucose (0.072 g), 4 nmol GOx (0.00064 g), and 2 μmol ammonium ferrous sulfate (0.00078 g) (all in acetate buffer) were added in the order mentioned to make up a total of 2 mL reaction solution in acetate buffer. A lid was placed on the glass vial and the reaction mixture was stirred at 200 rpm. The amounts mentioned are required for the synthesis of pDMA homopolymer with DP 100, with the following reagent concentrations: [DMA] = 1 M, [GOx] = 2 μM, [Iron-source] = 1 mM, [D-glucose] = excess. Reactions were conducted at room temperature for approximately 40–60 min and DP of polymerization was controlled by changing the ratio between mmol of monomer and RAFT agent, while keeping the monomer concentration constant. One-pot chain extension was then carried out by adding monomer and D-glucose stock solutions to the reaction mixture at appropriate intervals. For a typical chain extension (DP 50), 1 mmol DMA/NAM was added to the reaction mixture. 250 μL of a solution of D-glucose in acetate buffer (1 g in 10 mL buffer) was added to dilute the reaction mixture every two chain extensions to avoid high viscosity.

Automated multiblock copolymer synthesis using semi bio-Fenton RAFT Polymerization: Using the open access protocol designer tool available on the Opentrons website, a protocol for the desired number of chain extensions was designed and imported into the Opentrons app. After the manual preparation of the first block (macro-CTA), the glass vial containing the reaction solution was placed on a magnetic stirrer plate on the robot deck. Monomers and D-glucose stock solution were placed on the deck available for the robot to perform chain extensions by transferring the required volume of liquid reagents to the reaction solution. Chain extensions were normally performed for one hour, with samples taken by the robot for GPC and NMR analysis.

Characterization: Size-Exclusion Chromatography: Polymers were tested in an aqueous GPC/SEC to confirm molecular weight and polydispersity (Đ). MilliQ water with 0.1 vol% TFA was used as eluent at a flow rate of 1 mL.min^{-1}. Wyatt ASTRA SEC/LS software was used to calculate MW and Đ.

Nuclear Magnetic Resonance Spectroscopy: A Bruker Ascend 400 MHz NMR spectrometer was used to determine monomer conversion. Crude polymer samples were dissolved at a concentration of 10 mg mL^{-1} in either a 200 mM solution of hydroquinone in deuterated water (D_2O) or by simply diluting the reaction solution in D_2O to quench radical species. Monomer conversion was calculated via the integration of the vinyl peaks from the monomers (δ ~6.60-5.60 ppm) and comparing it to the integration from the polymer backbone (δ ~1.85-1.0 ppm).

Dynamic Light Scattering: DLS measurements were performed using a Malvern Nano Zetasizer. For each sample, three measurements were conducted at 25 °C at a scattering angle of 173°, and the average result was reported. All polymer samples were freeze-dried prior to dissolving in solvents at specific concentrations for DLS measurement.

Acknowledgements

V.J. is supported by the RTP (Research Training Program) Scholarship provided by the Australian Commonwealth Government and the University of Melbourne. V.J. would like to thank Omid Mazaheri for his help and insight in DLS measurement and data interpretation. Open Access publishing facilitated by The University of Melbourne, as part of the Wiley - The University of Melbourne agreement via the Council of Australian University Librarians.

Conflict of Interests

The authors declare no conflict of interest.

Data Availability Statement

The data that support the findings of this study are available from the corresponding author upon reasonable request.

Keywords: automation · block copolymers · chain-end fidelity · RAFT polymerization · sequence-control

[1] E. Ong, M. U. Wong, A. Huffman, Y. He, *Front. Immunol.* **2020**, *11*, 1581.
[2] F. Strieth-Kalthoff, F. Sandfort, M. H. S. Segler, F. Glorius, *Chem. Soc. Rev.* **2020**, *49*, 6154–6168.
[3] a) B. Burger, P. M. Maffettone, V. V. Gusev, C. M. Aitchison, Y. Bai, X. Wang, X. Li, B. M. Alston, B. Li, R. Clowes, N. Rankin, B. Harris, R. S. Sprick, A. I. Cooper, *Nature* **2020**, *583*, 237–241; b) S. V. Ley, D. E. Fitzpatrick, R. J. Ingham, R. M. Myers, *Angew. Chem. Int. Ed.* **2015**, *54*, 3449–3464; c) E. Stach, B. DeCost, A. G. Kusne, J. Hattrick-Simpers, K. A. Brown, K. G. Reyes, J. Schrier, S. Billinge, T. Buonassisi, I. Foster, C. P. Gomes, J. M. Gregoire, A. Mehta, J. Montoya, E. Olivetti, C. Park, E. Rotenberg, S. K. Saikin, S. Smullin, V. Stanev, B. Maruyama, *Matter* **2021**, *4*, 2702–2726; d) J. Yeow, R. Chapman, J. Xu, C. Boyer, *Polym. Chem.* **2017**, *8*, 5012–5022.
[4] a) S. Oliver, L. Zhao, A. J. Gormley, R. Chapman, C. Boyer, *Macromolecules* **2019**, *52*, 3–23; b) B. Lin, J. L. Hedrick, N. H. Park, R. M. Waymouth, *J. Am. Chem. Soc.* **2019**, *141*, 8921–8927; c) F. A. Leibfarth, J. A. Johnson, T. F. Jamison, *Proc. Nat. Acad. Sci.* **2015**, *112*, 10617–10622; d) Y. Zhou, Y. Gu, K. Jiang, M. Chen, *Macromolecules* **2019**, *52*, 5611–5617; e) C. Chen, F. Richter, J. Zhang, C. Guerrero-Sanchez, A. Traeger, U. S. Schubert, A. Feng, S. H. Thang, *Eur. Polym. J.* **2021**, *160*, 110777.
[5] M. Tamasi, S. Kosuri, J. DiStefano, R. Chapman, A. J. Gormley, *Adv. Intell. Syst.* **2020**, *2*, 1900126.
[6] a) M. Reis, F. Gusev, N. G. Taylor, S. H. Chung, M. D. Verber, Y. Z. Lee, O. Isayev, F. A. Leibfarth, *J. Am. Chem. Soc.* **2021**, *143*, 17677–17689; b) M. J. Tamasi, R. A. Patel, C. H. Borca, S. Kosuri, H. Mugnier, R. Upadhya, N. S. Murthy, M. A. Webb, A. J. Gormley, *Adv. Mater.* **2022**, *34*, 2201809; c) S. T. Knox, S. J. Parkinson, C. Y. P. Wilding, R. A. Bourne, N. J. Warren, *Polym. Chem.* **2022**, *13*, 1576–1585; d) J. Van Herck, I. Abeysekera, A.-L. Buckinx, K. Cai, J. Hooker, K. Thakur, E. Van de Reydt, P.-J. Voorter, D. Wyers, T. Junkers, *Digit. Discov.* **2022**, *1*, 519–526.
[7] a) M. Rubens, J. H. Vrijsen, J. Laun, T. Junkers, *Angew. Chem. Int. Ed.* **2019**, *58*, 3183–3187; b) M. Rubens, J. Van Herck, T. Junkers, *ACS Macro Lett.* **2019**, *8*, 1437–1441.
[8] T. B. Martin, D. J. Audus, *ACS Polym. Au* **2023**, *3*, 239–258.
[9] a) C. Boyer, V. Bulmus, T. P. Davis, V. Ladmiral, J. Liu, S. Perrier, *Chem. Rev.* **2009**, *109*, 5402–5436; b) B. Charleux, G. Delaittre, J. Rieger, F. D'Agosto, *Macromolecules* **2012**, *45*, 6753–6765; c) M. R. Hill, R. N. Carmean, B. S. Sumerlin, *Macromolecules* **2015**, *48*, 5459–5469; d) J.-F. Lutz, *ACS Macro Lett.* **2014**, *3*, 1020–1023.
[10] a) C. Guerrero-Sanchez, S. Harrisson, D. J. Keddie, *Macromol. Symp.* **2013**, *325-326*, 38–46; b) C. Guerrero-Sanchez, R. M. Paulus, M. W. M. Fijten, M. J. de la Mar, R. Hoogenboom, U. S. Schubert, *Appl. Surf. Sci.* **2006**, *252*, 2555–2561; c) D. Fournier, R. Hoogenboom, H. M. L. Thijs, R. M. Paulus, U. S. Schubert, *Macromolecules* **2007**, *40*, 915–920; d) C. Guerrero-Sanchez, D. J. Keddie, S. Saubern, J. Chiefari, *ACS Comb. Sci.* **2012**, *14*, 389–394.
[11] X. Pan, S. Lathwal, S. Mack, J. Yan, S. R. Das, K. Matyjaszewski, *Angew. Chem. Int. Ed.* **2017**, *56*, 2740–2743.
[12] J. Lee, P. Mulay, M. J. Tamasi, J. Yeow, M. M. Stevens, A. J. Gormley, *Digit. Discov.* **2023**, *2*, 219–233.

[13] H. Foster, M. H. Stenzel, R. Chapman, *Macromolecules* **2022**, *55*, 5938–5945.
[14] a) A. H. Soeriyadi, C. Boyer, F. Nyström, P. B. Zetterlund, M. R. Whittaker, *J. Am. Chem. Soc.* **2011**, *133*, 11128–11131; b) N. G. Engelis, A. Anastasaki, G. Nurumbetov, N. P. Truong, V. Nikolaou, A. Shegiwal, M. R. Whittaker, T. P. Davis, D. M. Haddleton, *Nat. Chem.* **2017**, *9*, 171–178.
[15] G. Gody, T. Maschmeyer, P. B. Zetterlund, S. Perrier, *Nat. Commun.* **2013**, *4*, 2505.
[16] F. S. Bates, M. A. Hillmyer, T. P. Lodge, C. M. Bates, K. T. Delaney, G. H. Fredrickson, *Science* **2012**, *336*, 434–440.
[17] C. M. Bates, F. S. Bates, *Macromolecules* **2017**, *50*, 3–22.
[18] A. S. Abd-El-Aziz, M. Antonietti, C. Barner-Kowollik, W. H. Binder, A. Böker, C. Boyer, M. R. Buchmeiser, S. Z. D. Cheng, F. D'Agosto, G. Floudas, H. Frey, G. Galli, J. Genzer, L. Hartmann, R. Hoogenboom, T. Ishizone, D. L. Kaplan, M. Leclerc, A. Lendlein, B. Liu, T. E. Long, S. Ludwigs, J.-F. Lutz, K. Matyjaszewski, M. A. R. Meier, K. Müllen, M. Müllner, B. Rieger, T. P. Russell, D. A. Savin, A. D. Schlüter, U. S. Schubert, S. Seiffert, K. Severing, J. B. P. Soares, M. Staffilani, B. S. Sumerlin, Y. Sun, B. Z. Tang, C. Tang, P. Théato, N. Tirelli, O. K. C. Tsui, M. M. Unterlass, P. Vana, B. Voit, S. Vyazovkin, C. Weder, U. Wiesner, W.-Y. Wong, C. Wu, Y. Yagci, J. Yuan, G. Zhang, *Macromol. Chem. Phys.* **2020**, *221*, 2000216.
[19] a) D. J. Keddie, *Chem. Soc. Rev.* **2014**, *43*, 496–505; b) M. G. T. A. Rutten, F. W. Vaandrager, J. A. A. W. Elemans, R. J. M. Nolte, *Nat. Chem. Rev.* **2018**, *2*, 365–381; c) P. R. Judzewitsch, T.-K. Nguyen, S. Shanmugam, E. H. H. Wong, C. Boyer, *Angew. Chem. Int. Ed.* **2018**, *57*, 4559–4564; d) D. Chan-Seng, M. Zamfir, J.-F. Lutz, *Angew. Chem. Int. Ed.* **2012**, *51*, 12254–12257; e) J.-F. Lutz, M. Ouchi, D. R. Liu, M. Sawamoto, *Science* **2013**, *341*, 1238149.
[20] a) A. J. Gormley, J. Yeow, G. Ng, Ó. Conway, C. Boyer, R. Chapman, *Angew. Chem. Int. Ed.* **2018**, *57*, 1557–1562; b) R. Chapman, A. J. Gormley, M. H. Stenzel, M. M. Stevens, *Angew. Chem. Int. Ed.* **2016**, *55*, 4500–4503; c) C. Zhang, M. W. Bates, Z. Geng, A. E. Levi, D. Vigil, S. M. Barbon, T. Loman, K. T. Delaney, G. H. Fredrickson, C. M. Bates, A. K. Whittaker, C. J. Hawker, *J. Am. Chem. Soc.* **2020**, *142*, 9843–9849.
[21] a) G. Polymeropoulos, G. Zapsas, K. Ntetsikas, P. Bilalis, Y. Gnanou, N. Hadjichristidis, *Macromolecules* **2017**, *50*, 1253–1290; b) N. Hadjichristidis, H. Iatrou, M. Pitsikalis, S. Pispas, A. Avgeropoulos, *Prog. Polym. Sci.* **2005**, *30*, 725–782; c) R. J. Spontak, J. C. Fung, M. B. Braunfeld, J. W. Sedat, D. A. Agard, L. Kane, S. D. Smith, M. M. Satkowski, A. Ashraf, D. A. Hajduk, S. M. Gruner, *Macromolecules* **1996**, *29*, 4494–4507; d) J. N. L. Albert, T. H. Epps, *Mater. Today* **2010**, *13*, 24–33; e) F. Wurm, H. Frey, *Prog. Polym. Sci.* **2011**, *36*, 1–52; f) Y. Bai, H. Wang, J. He, Y. Zhang, *Angew. Chem. Int. Ed.* **2020**, *59*, 11613–11619; g) A. Anastasaki, B. Oschmann, J. Willenbacher, A. Melker, M. H. C. Van Son, N. P. Truong, M. W. Schulze, E. H. Discekici, A. J. McGrath, T. P. Davis, C. M. Bates, C. J. Hawker, *Angew. Chem. Int. Ed.* **2017**, *56*, 14483–14487; h) M. Steube, T. Johann, E. Galanos, M. Appold, C. Rüttiger, M. Mezger, M. Gallei, A. H. E. Müller, G. Floudas, H. Frey, *Macromolecules* **2018**, *51*, 10246–10258; i) G. Gody, T. Maschmeyer, P. B. Zetterlund, S. Perrier, *Macromolecules* **2014**, *47*, 3451–3460; j) G. K. K. Clothier, T. R. Guimarães, G. Moad, P. B. Zetterlund, *Macromolecules* **2022**, *55*, 1981–1991; k) T. Stößer, D. Mulryan, C. K. Williams, *Angew. Chem. Int. Ed.* **2018**, *57*, 16893–16897; l) A. C. Deacy, G. L. Gregory, G. S. Sulley, T. T. D. Chen, C. K. Williams, *J. Am. Chem. Soc.* **2021**, *143*, 10021–10040.
[22] V. P. Beyer, J. Kim, C. R. Becer, *Polym. Chem.* **2020**, *11*, 1271–1291.
[23] a) A. Reyhani, M. D. Nothling, H. Ranji-Burachaloo, T. G. McKenzie, Q. Fu, S. Tan, G. Bryant, G. G. Qiao, *Angew. Chem. Int. Ed.* **2018**, *57*, 10288–10292; b) A. Reyhani, S. Allison-Logan, H. Ranji-Burachaloo, T. G. McKenzie, G. Bryant, G. G. Qiao, *J. Polym. Sci. Part A* **2019**, *57*, 1922–1930.
[24] M. H. Reis, F. A. Leibfarth, L. M. Pitet, *ACS Macro Lett.* **2020**, *9*, 123–133.
[25] N. Corrigan, K. Jung, G. Moad, C. J. Hawker, K. Matyjaszewski, C. Boyer, *Prog. Polym. Sci.* **2020**, *111*, 101311.
[26] Z. An, *ACS Macro Lett.* **2020**, *9*, 350–357.
[27] a) A. Reyhani, T. G. McKenzie, Q. Fu, G. G. Qiao, *Macromol. Rapid Commun.* **2019**, *40*, 1900220; b) C. M. Wong, K. H. Wong, X. D. Chen, *Appl. Microbiol. Biotechnol.* **2008**, *78*, 927–938.
[28] R. Upadhya, S. Kosuri, M. Tamasi, T. A. Meyer, S. Atta, M. A. Webb, A. J. Gormley, *Adv. Drug Delivery Rev.* **2021**, *171*, 1–28.
[29] a) P. Alexandridis, R. J. Spontak, *Curr. Opin. Colloid Interface Sci.* **1999**, *4*, 130–139; b) Y. Mai, A. Eisenberg, *Chem. Soc. Rev.* **2012**, *41*, 5969–5985; c) Z. Li, Z. Lin, *Polym. Int.* **2022**, *71*, 366–370; d) C. Lv, J. Gao, K. An, J. Nie, J. Xu, B. Du, *Macromolecules* **2021**, *54*, 6489–6501; e) Y. Liu, F. Ke, Y. Li, Y. Shi, Z. Zhang, Y. Chen, *Nano Res.* **2023**, *16*, 564–582; f) A. B. Chang, C. M. Bates, B. Lee, C. M. Garland, S. C. Jones, R. K. W. Spencer, M. W. Matsen, R. H. Grubbs, *Proc. Nat. Acad. Sci.* **2017**, *114*, 6462–6467; g) L. Guo, J. Xu, B. Du, *Polym. Rev.* **2023**, 1–35; h) M. Karayianni, S. Pispas, *J. Polym. Sci.* **2021**, *59*, 1874–1898.
[30] S. Ji, M. Lin, Z. Li, L. Xu, X. Fu, G. Chen, Z. Li, J. Sun, *Biomacromolecules* **2022**, *23*, 798–807.
[31] F. Ke, X. Mo, R. Yang, Y. Wang, D. Liang, *Macromolecules* **2009**, *42*, 5339–5344.
[32] Y. Yu, A. Eisenberg, *J. Am. Chem. Soc.* **1997**, *119*, 8383–8384.
[33] H. M. L. Lambermont-Thijs, R. Hoogenboom, C.-A. Fustin, C. Bomal-D'Haese, J.-F. Gohy, U. S. Schubert, *J. Polym. Sci. Part A* **2009**, *47*, 515–522.
[34] Y. S. Jo, A. J. van der Vlies, J. Gantz, S. Antonijevic, D. Demurtas, D. Velluto, J. A. Hubbell, *Macromolecules* **2008**, *41*, 1140–1150.
[35] A. Choucair, A. Eisenberg, *Eur. Phys. J. E* **2003**, *10*, 37–44.
[36] X. Qiang, R. Chakroun, N. Janoszka, A. H. Gröschel, *Isr. J. Chem.* **2019**, *59*, 945–958.

Manuscript received: June 2, 2023
Accepted manuscript online: July 3, 2023
Version of record online: July 3, 2023